Dalton Transactions

Accepted Manuscript

ROYAL SOCIETY OF CHEMISTRY

rsc.li/dalton

View Article Online
DOI: 10.1039/C8DT02140F

Journal Name

ARTICLE

Dinuclear iminophenoxide copper complexes in *rac*-Lactide polymerisation

Received 00th January 20xx,
Accepted 00th January 20xx

DOI: 10.1039/x0xx00000x

www.rsc.org/

Pargol Daneshmand,[a] Leena Pinon,[a] Frank Schaper[a,*]

Dinuclear bis(R'-(R"-iminomethyl)phenoxide) copper complexes $L_2Cu_2(\mu\text{-}OR)_2$ were prepared from the reaction of copper methoxide with ROH and LH (ROH = dimethylaminoethanol or pyridylmethanol, R' = H, 4,6-*t*Bu, 1,3-Cl, R" = benzyl, cyclohexyl, diphenylmethyl and 2,6-dimethylphenyl). Preparation was complicated by formation of homoleptic L_2Cu and only 9 of the 24 possible combinations could be prepared. All complexes were characterized by single crystal X-ray diffraction studies and crystallized as dinuclear penta-coordinated complexes. Homoleptic complexes L_2Cu were inactive in lactide polymerization at room temperature. Most heteroleptic complexes showed modest to good activities with full conversion in less than 6 h at room temperature. Complexes with R'=H showed poor molecular weight control, complexes with R'=Cl were inactive in polymerization. In pyridylmethoxide-containing complexes, only one alkoxide initiated chain growth. All complexes produced atactic polymer.

Introduction

In the interest to find sustainable replacements for petroleum-based resources, polylactic acid (PLA) is considered an alternative to polyolefin-based plastics. PLA is obtained by the ring-opening polymerization of lactide, the dimeric anhydride of lactic acid, obtained from the fermentation of corn starch.[1-11] Although lactide is not difficult to polymerize, combining high polymerization activity with good polymerization control poses a catalytic challenge and attracted academic interest in developing improved catalyst systems, most often based on a coordination-insertion mechanism.[12-38] With regard to stereocontrol, *rac*-lactide has a high tendency towards alternating monomer insertion and highly heterotactic PLA ($\{RR\text{-}SS\}_n$, P_m = 0, Scheme 1) was obtained already in early

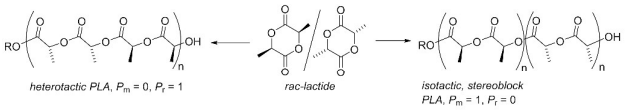

Scheme 1

work of Coates on diketiminate zinc catalysts.[39] To obtain the industrially relevant isotactic PLA ($\{RR\}_n/\{SS\}_n$ or$\{RR\}_n\{SS\}_n$, P_m = 1) in combination with high activity and good polymer molecular weight control, was more challenging. Although promising catalyst systems have emerged,[40-49] their optimization remains hindered by the tendency of lactide-polymerization catalysts to react with sometimes catastrophic changes in reactivity upon modification of the ligand framework.

[a] *Centre in Green Chemistry and Catalysis, Department of chemistry, Université de Montréal, C. P. 6128 Succ. Centre-Ville, Montréal, QC, H3T 3J7, Canada.*
* Email: Frank.Schaper@umontreal.ca
Electronic Supplementary Information (ESI) available: Additional graphics and tables, NMR spectra of ligands, and details of X-ray diffraction analysis (CIF).

View Article Online
DOI: 10.1039/C8DT02140F

Of metal-based catalysts for coordination-insertion polymerization of lactide, d^0- and d^{10} metals received the highest attention, while catalysts based on groups 5-11 remained largely unexplored. There are very few reports of catalysts based on Cr,[46] Mn,[50-54] Ni,[55-59] or Co.[52, 60-62] None of these systems could compete in stereocontrol or activity with d^0- or d^{10}-metal based catalysts. Complexes based on iron and copper have been studied in somewhat more detail. Several iron complexes showed high activity for coordination-insertion polymerization[63-68] and polymerization activity of iron complexes can be turned on or off by switching their redox state.[69, 70] A recent study reported the first isotactic PLA obtained with iron-based complexes.[71] Copper-based polymerization catalysts are the 2nd largest group investigated. The catalysts were either carboxylate salts,[72-74] homoleptic complexes with iminophenoxide-based ligands,[55, 75, 76] or copper(II) salen complexes.[77, 78] None of these complexes were optimized for coordination-insertion polymerization and the sterically saturated copper centers are not expected to be highly Lewis-acidic. Thus in general only low activities were observed, even in molten polymer. Polymer molecular weight control was often excellent, on the other hand. The one exception with regard to low activities is a copper salen complex, which showed, in the presence of benzyl alcohol, surprising activity in solution (24 h at RT).[78] In 2012, we reported that heteroleptic diketiminate copper(II) alkoxides showed very high activity in *rac*-lactide polymerization in solution (<5 min at RT).[79-81] Perfect molecular weight control, the absence of side reactions, and – unfortunately – also of stereocontrol characterized these catalysts. Jeong's group reported similarly high activities for *in-situ* generated diamino- or pyridylamino copper(II) alkoxide complexes.[82-86] PLA obtained with these complexes was highly heterotactic, the first time notable stereocontrol was observed in copper-catalyzed lactide polymerization. In 2015, we reported that heteroleptic iminopyrrolide copper alkoxide complexes polymerized lactide with a preference for isotactic monomer insertion, the first time isotactic lactide polymerization was observed for a Cu-based catalyst.[87] The active species is dinuclear and one of the initial pyridylmethoxide ligands does not initiate polymerization, but is retained as a spectator ligand in t1 he complex (Scheme 2).[88, 89] The nature of the bridging alkoxide ligand proved to be crucial for stereocontrol and a major impediment in catalyst optimization: Bridges less "rigid" than pyridylmethoxide, such as pyridylethoxide or dimethylaminoethoxide led to loss of stereocontrol. With dimethylaminoethoxide, both alkoxides initiated chain growth. More rigid bridges, such as iminoaryloxides or hydroxyquinoline led to loss of activity (Scheme 2).[88]

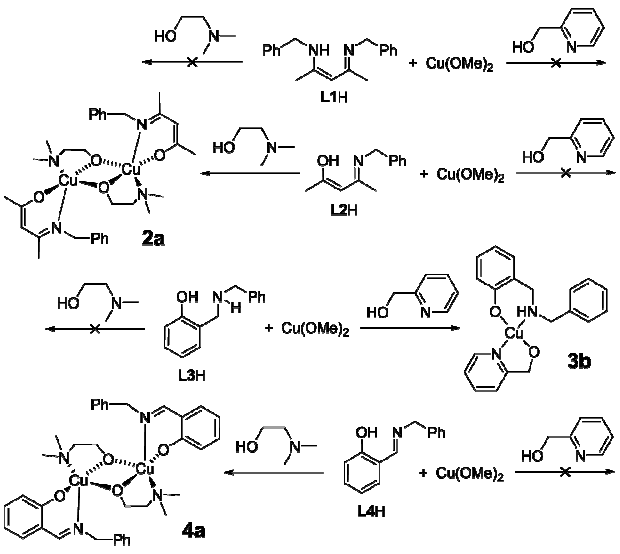

Scheme 3

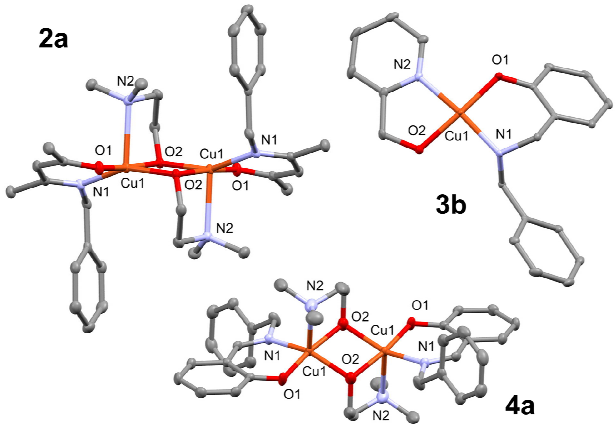

Figure 1. X-ray structures of **2a**, **3b** and **4a**. Thermal displacements are shown at the 50% probability level. Hydrogen atoms and the minor part of the aminoethoxide disorder in **4a** were omitted for clarity.

View Article Online
DOI: 10.1039/C8DT02140F

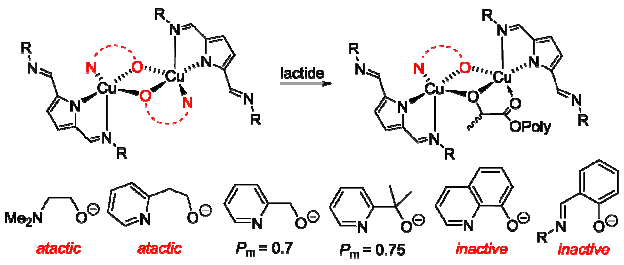

Scheme 2

Since stereocontrol seemed to rely on the presence of a pyridylmethoxide bridging ligand, we turned our attention towards possible variations of the spectator ligand. In the following, we describe the preparation of dinuclear pyridylmethoxide complexes with spectator ligands other than iminopyrrolides, in particular heteroleptic iminophenoxide complexes, and their application in the *rac*-lactide polymerization.

Results and discussion

Four different ligand systems similar to iminopyrroles were targeted for initial exploration in form of their *N*-benzyl substituted derivatives: β-diketimines, β-aminoketones, aminophenols, and iminophenols (Scheme 3). We were not able to prepare any heteroleptic copper complexes from the reaction of copper methoxide with **L1**H in the presence of either dimethylaminoethanol or pyridylmethanol. Reactions either yielded unidentifiable mixtures or the known homoleptic complex (**L1**)$_2$Cu.[80] Reactions with **L2**H in the presence of dimethylaminoethanol yielded the dinuclear complex **2a** (Scheme 3). No product was obtained with pyridylmethoxide or when the *N*-substituent was cyclohexyl, diphenylmethyl, or xylyl. Complex **2a** crystallized as an aminoalkoxide-bridged dimer (Fig. 1, Table 1). The coordination geometry around copper is square-pyramidal, with a τ-value of 0.3.[90] The amine nitrogen is found in the apical position. Cu-N/O bond distances of 1.93-1.99 Å are unremarkable for equatorial atoms in square-pyramidal Cu(II) complexes.

Table 1 Bond distances [Å] in crystal structures of **2a**, **3b** and **4a**

	2a	**3b**	**4a**
Cu-O1 (ligand)	1.930(1)	1.915(1)	1.913(1) [a]
Cu-N1 (ligand)	1.988(1)	2.029(1)	1.995(2) [a]
Cu-O2$_{short}$ (alkoxide)	1.966(1)	1.929(1)	1.956(2) [a]
Cu-O2$_{long}$ / Cu-N3	1.991(1)	2.512(1)	2.029(1) [a]
Cu-N2	2.341(1)	1.992(1)	2.289(2)
Cu-Cu	2.9922(4)		3.0027(5)
τ	0.3	0.1	0.3
Ligand in apical position	Amine	Pyridylmethanol	Amine

[a] Data only shown for major part of dimethylaminoethoxide disorder.

View Article Online
DOI: 10.1039/C8DT02140F

Complex **2a** was active in *rac*-lactide polymerization and reached full conversion in appr. 5 h (Table 2). The reaction followed pseudo-first-order kinetics (Fig. S1). As expected for catalyst with an aminoethoxide bridging ligand, the obtained PLA was atactic. We have shown previously that pyridylmethoxide complexes with isotactic stereocontrol can be formed *in situ* from the respective aminoethoxide complexes, which showed no stereocontrol by addition of pyridylmethanol to the polymerization reaction.[87-89] *rac*-Lactide was thus polymerized with **2a** in the presence of 1 equiv pyridylmethanol. However no change in the stereochemistry of the polymer was observed (Table 2). Polymerizations with **2a** and **2a**/$PyCH_2OH$ both showed poor polymer molecular weight control, with polydispersities of 1.7-2.6 and lower than expected polymer molecular weights. It was thus not possible to determine whether added $PyCH_2OH$ served as a simple chain-transfer reagent in immortal polymerization or whether it was incorporated as a spectator ligand, but without providing stereocontrol. The activity of **2a** was appr. twice as high in the presence of $PyCH_2OH$. While not investigated in detail, the negative *x*-axis intercept in polymerization with **2a** indicates a fast catalyst deactivation at the start of the reaction, which was suppressed in the presence of pyridylmethanol (Fig. S1).

Reaction of the aminophenol ligand **L3**H with copper methoxide in the presence of pyridylmethanol afforded complex **3b** (Scheme 1), which crystallized as a monomeric complex with the square-pyramidal geometry completed by a ancillary pyridylmethanol ligand (Fig. 1, Table 1). Cu-N/O bond distances are in the expected range. Compared to Cu-N_{imino} bond distances (where the *N*-substituent is benzyl), the Cu-N_{amino} bond distance is longer by appr. 0.3 Å, as expected for an sp^3- vs. sp^2-donor ligand. Complex **3b** was essentially inactive for lactide polymerization at room temperature, and reacted sluggishly even at 50 °C (Table 2). The obtained PLA was moderately heterotactic (P_m = 0.23), but due to possible

Table 2 *Rac*-lactide polymerizations [a]

Entry	Catalyst	Final conversion	k_{obs} [h^{-1}]	M_n [b]	M_n (calc.) [c]	M_w/M_n	# chains [d]	P_m [e]
1	**2a**	97%	0.31(2)	4.3 kDa	14.0 kDa	1.7	3.3	0.48
2	**2a** + 1 PyCH2OH	99%	0.61(2)	2.4 kDa	14.1 kDa	2.6	5.8	0.48
3	**3b**	3%	-	-	-	-	-	-
4	**3b** (at 50 °C)	24%	-	0.8 kDa	3.5 kDa	1.3	4.4	0.23
6	**4a**	96%	0.60(0)	7.7 kDa	13.8 kDa	1.2	1.8	0.53
5	**4c** + 5 BnOH	0%	-	-	-	-	-	-
7	**5a**	99%	0.80(1)	5.5 kDa	14.3 kDa	1.5	2.6	0.5
8	**5a**+ 1 $PyCH_2OH$	97%	1.07(3)	4.3 kDa	14.0 kDa	1.5	3.2	0.49
9	**6a**	36%	-	6.9 kDa	5.2 kDa	1.3	1	0.43
10	**6b**	26%	-	1.4 kDa	3.7 kDa	1.3	2.6	0.35
13	**8b**	97%	0.56(8)	14.5 kDa	14.0 kDa	1.2	1	0.53
15	**9a**	98%	0.82(3)	7.5 kDa	14.1 kDa	1.1	1.9	0.48
16	**9a** + 1 $PyCH_2OH$	99%	1.8(0)	4.8 kDa	14.1 kDa	1.2	2.9	0.48
14	**11b**	98%	1.05(12)	15.3 kDa	14.1 kDa	1.3	1.1	0.50
17	**12b**	13%	-	-	-	-	-	-
11	**16a**	15%	-	-	14.4 kDa	-	-	-
12	**16b**	3%	-	-	14.4 kDa	-	-	-

[a] Conditions: C_6D_6, RT, [lactide] = 200 mM, $[L_2Cu_2(OR)_2]$ = 2 mM. [b] M_n and M_w determined by size exclusion chromatography vs. polystyrene standards, with a Mark-Houwink correction factor of 0.58. [c] M_n expected if one alkoxide per catalyst dimer initiates polymerization, calculated from [lactide]/[cat]·conversion·$M_{lactide}$ + M_{ROH}. [d] Number of chains per catalyst dimer, calculated from the ratio of expected and obtained polymer molecular weight. [e] P_m determined from decoupled ^{1}H NMR by $P_m = 1 - 2 \cdot I_1/(I_1+I_2)$, with I_1 = 5.20 – 5.25 ppm (*rmr, mmr/rmm*), I_2 = 5.13 – 5.20 ppm (*mmr/rmm, mmm, mrm*).

View Article Online
DOI: 10.1039/C8DT02140F

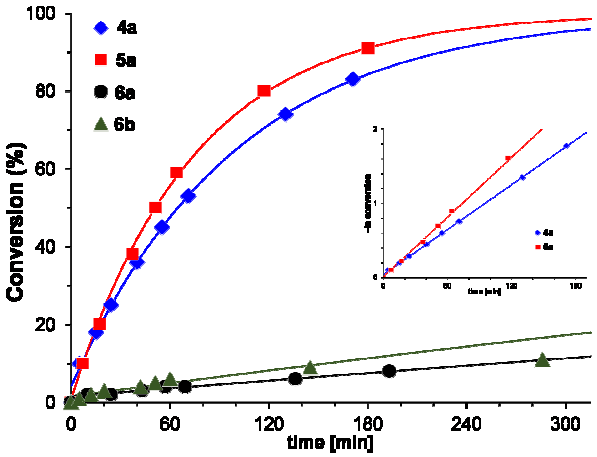

Figure 2. Conversion-time profiles for rac-lactide polymerization with **4a** (diamonds), **5a** (squares, **6a** (circles) and **6b** (triangles). Conditions: C_6D_6, RT, 0.2 M lactide, 2 mM [cat.]. The inset shows the semi-logarithmic plot. Solid lines represent in both graphics theoretical conversions with the values obtained in linear regression analysis: **4a**: k_{app} = 0.604(2) h^{-1}, t_0 = –4 min, **5a**: k_{app} = 0. 0.80(1) h^{-1}, t_0 = –1 min.

complex decomposition and the lower than expected polymer molecular weight, the reaction mechanism and the active species are unclear. The inactivity of **3b** in polymerization is not due to coordination of pyridylmethanol, which can be added as an external alcohol to polymerizations without any loss of activity. It correlates better with the fact that **3b** crystallized as a monomeric, pyridine-coordinated complex. All copper catalysts isolated in our laboratories which showed high activities in coordination-insertion polymerization of lactide formed alkoxide-bridged dimers in the solid state, although excess pyridylmethanol was always present in the reaction mixture. The amino-phenoxide ligand seems to reduce the Lewis acidity of copper sufficiently to discourage the coordination of a bridging alkoxide and likewise of lactide monomer.

Unlike its amino-derivative, we were unable to obtain pyridylmethoxide complexes with the iminophenol ligand **L4**H. Instead, the respective homoleptic complex **4c**, $(\mathbf{L4})_2$Cu,[91, 92] was obtained (*vide infra*). The respective aminoethoxide complex, **4a**, could be prepared readily. Complex **4a** crystallizes as the expected dimeric complex with a square-pyramidal coordination around copper and the amine ligand in the apical position (Fig. 1, Table 1).

Since surprisingly high room temperature activity was reported for a copper(II) salen complex following an activated monomer mechanism,[78] the homoleptic complex **4c** was employed for lactide polymerization in the presence of 5 equiv of benzyl alcohol. However, no activity was observed (Table 2). The iminophenol ligand is too acidic to be protonated in sufficient amounts to form active, heteroleptic species,[81] and the complex is not Lewis-acidic enough to catalyse polymerization via an activated monomer mechanism. The heteroleptic complex, on the other hand, showed good activity in lactide polymerization with full conversion in less than 5 h at room temperature. Polymerizations with **4a** followed clean first-order kinetics (Fig. 2), without any notable induction period or catalyst decomposition. The polydispersity was narrow (M_w/M_n = 1.2) and the polymer molecular weight is in good agreement with both alkoxides initiating chain growth. As expected for a catalyst with an aminoethoxide bridging ligand,[87-89] the obtained polymer was atactic.

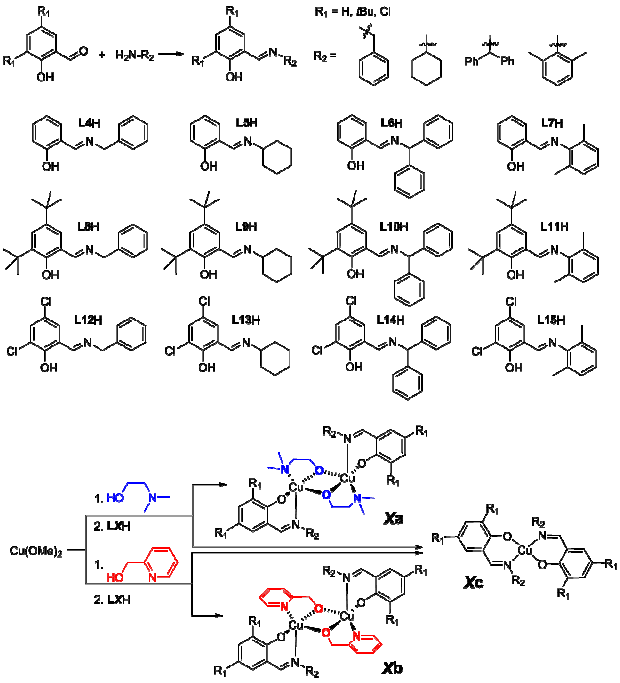

Scheme 4

Iminophenols - ligand and general complex synthesis.

Given the good activity and stereocontrol observed for **4a**, we decided to further explore iminophenol ligands for the coordination-insertion polymerization of lactide. All iminophenol ligands, if not already reported, were synthesized through condensation of the salicylaldehyde derivative with the respective amine, based on a previously reported method (Scheme 4, Exp. section).[88] Dinuclear copper complexes $\{LCu(\mu OR)\}_2$ were obtained by successive addition of aminoalcohol and the respective iminophenol ***L*X**H to a solution of copper methoxide. Initial addition of (excess) aminoalcohol led to a blue solution. Reaction with the ligand typically formed green solutions, from which the heteroleptic complex with either a dimethylaminoethoxide, ***X*a**, or pyridylmethoxide, ***X*b**, bridging ligand could be crystallized (Scheme 4). Control of the Schlenk equilibrium proved to be very difficult for iminophenol ligands. In most cases (*vide infra*), dark-brown solutions were obtained after reaction with iminophenol and crystallization – if successful – afforded the homoleptic complexes, ***X*c** (Scheme 4), typically as brown crystals and sometimes accompanied by the respective bisaminoalkoxide complex (Fig. S2). Variations of reaction conditions, such as changes of solvent, stoichiometry or order

View Article Online
DOI: 10.1039/C8DT02140F

of addition, did not improve the reaction outcome in any of these cases.

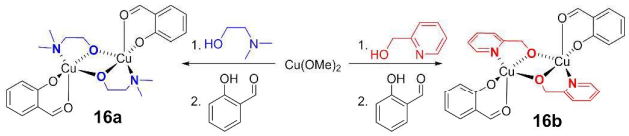

Scheme 5

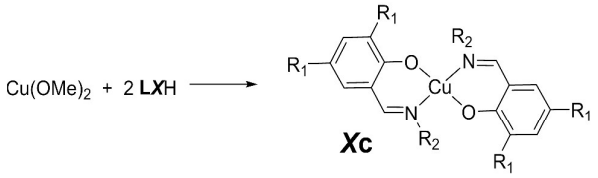

Scheme 6

Salicylaldehyde-based ligands.

Analogous to **4a**, reaction of copper(II) methoxide with two equiv of dimethylaminoethanol, followed by addition of the iminophenol ligand lead to green solutions, from which the heteroleptic complexes **5a** and **6a** crystallized. With the sterically demanding xylyl *N*-substituent, only the homoleptic complex **7c** was obtained. Formation of homoleptic complexes was even more pronounced with the pyridylmethoxide ligand: only with a diphenylmethyl *N*-substituent, **L6**H, the heteroleptic complex **6b** was obtained. Reactions of **L4**H, **L5**H, or **L7**H afforded dark-brown solutions and after crystallization the homoleptic complexes L_2Cu **4c**, **5c** and **7c**. We have noted before that introduction of a pyridylmethoxide bridging ligand is sterically more demanding than that of a dimethylaminoethoxide ligand.[89] Indeed, if salicylaldehyde was used as spectator ligand, i. e. in the absence of any *N*-substituent, copper complexes **16a** and **16b** were obtained with both bridging ligands (Scheme 5, Fig. 3). Homoleptic complexes **4c**-**7c** were prepared independently from reaction of copper(II) methoxide with two equivalents of iminophenol for characterization purposes (Scheme 6, Fig. S2). Preparation of **6c** was straightforward and occurred with a yield similar to the other homoleptic complexes. The formation of **6b** is thus not due to an inaccessibility of the homoleptic complex.

As does **4a**, heteroleptic complexes **5a**, **6a**, **6b**, **16a** and **16b** crystallize as dinuclear complexes with bridging aminoalkoxide ligands and with copper in a square-pyramidal geometry (Fig. 3, Table 3). The latter is confirmed by τ-values of 0.3 for all complexes.[90] Consequently, four ligands are found in the equatorial plane with bond distances of appr. 1.9 – 2.0 Å, while one ligand occupies the apical position with an elongated distance of 2.2 – 2.3 Å to the copper center. In **4a**-**6a** the amino group of the bridging ligand occupies the apical position and in **16a+b** the keto-group of salicylaldehyde. In **6b**, on the other hand, the bridging alkoxide is found in the apical position. The structural data does not offer any indication why placement of the alkoxide in the apical position should be favoured for **6b**. It should be noted, however, that a bridging alkoxide is likewise observed in the copper bis(pyridylmethoxide) dimer (Fig. S3). Placement of the anionic bridging alkoxide in the weak apical coordination site is thus not a simple consequence of the steric bulk of the diphenylmethyl *N*-substituent. Copper-oxygen and copper-nitrogen distances are in the range expected for five-coordinated Cu(II) complexes.[93] The steric bulk of the *N*-substituent is notable in a Cu-N_{imine} distance > 2.0 Å in **6a** and **6b**, while it remains <2.0 Å in **4a** and **5a**.

All heteroleptic complexes were active for the polymerization of lactide at room temperature in C_6D_6 solution (Table 2). Under typical conditions (2 mM cat., 200 mM *rac*-lactide), polymerizations with **4a** and **5a** reached completion in less then 5 h (Table 2). Polymerizations followed a pseudo-first order rate law with comparable apparent rate constants for both catalysts. Only a negligible induction period was observed

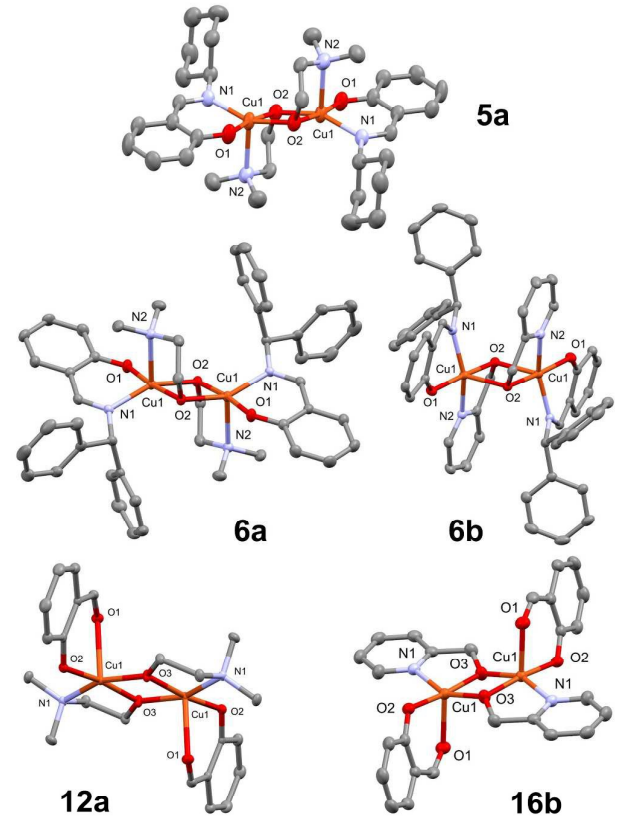

Figure 3. X-ray structures of **5a**, **6a**, **6b**, and **16a** and **16b**. Thermal displacements are shown at the 50% probability level. Hydrogen atoms were omitted for clarity. Only one of two independent molecules shown for **5a**.

View Article Online
DOI: 10.1039/C8DT02140F

before the start of the polymerization (Fig. 2). Both complexes provided atactic PLA, which is in agreement with results from iminopyrrolide copper complexes, which require the presence of a pyridylmethoxide bridging ligand for isotacticity. Addition of one equivalent of pyridylmethoxide to polymerizations with **5a**, in an attempt to generate **5b** *in situ*, was well tolerated, but did not influence stereocontrol. Complexes **6a** and **6b** reacted only sluggishly and even after 3 days, conversions did not surpass 36% and 26%, respectively (Table 2). Salicylaldehyde complexes **16a** and **16b** were essentially unreactive at room temperature. Contrary to **4a** and **5a**, polymerizations with **6a** and **6b** were moderately heterotactic. The latter might be a consequence of the increased steric bulk of the *N*-substituent or – more likely considering also their low activity – indicative of complex decomposition. The good polymer molecular weight control observed for **4a** is unfortunately not retained for its derivatives. Complexes **5a**, **6a**, and **6b** show only mediocre polymer molecular weight control, with polydispersities ranging from 1.3 to 1.5 (Table 2). Based on the polymerization behaviour in the analogous iminopyrrolide complexes, we expected only one pyridylmethoxide substituent per catalyst dimer to initiate polymerization, while both aminoethoxide groups should initiate. The low polymer molecular weight control prevents any conclusion whether the same initiator behaviour is followed in iminophenoxide complexes.

4,6-di(*tert*-butyl)salicylaldehyde-based ligands.

To improve polymer molecular weight control, we investigated iminophenols carrying *tert*-butyl substituents in *ortho*- and *para*-position. As for the salicylaldehyde-based ligands, dimethylaminoethoxide complexes **9a** and **10a** could be obtained with *N*-cyclohexyl and *N*-diphenylmethyl substituents. Only trace amounts were obtained for **10a**, however, which was thus not employed in polymerization. The respective pyridylmethoxide complexes were inaccessible. Surprisingly, the inverse was true for the sterically less demanding *N*-benzyl containing ligand, as well as the sterically more bulky *N*-xylyl ligand, where we could obtain the pyridylmethoxide containing complexes **8b** and **11b**, but not the respective aminoethoxide complexes. In contrast to salicylaldehyde-based ligands, homoleptic complexes were not obtained as alternative reaction products, although the preparations and structures of **8c**,[94] **9c**,[94] and **11c**[95, 96] have been reported in the literature. Previous preparations of heteroleptic LCu(OR) complexes indicated β-hydride elimination from the alkoxide, followed by decomposition of the Cu(II) hydride as a secondary reaction pathway, in particular for sterically demanding ligands.[80, 89] In some cases Cu(I) reaction products have been isolated,[89] in others not.[80] A similar decomposition pathway via β-hydride elimination might be in place here.

All isolated complexes crystallized again as dimers with bridging alkoxide ligands (Fig. 4, Table 3) and a square-pyramidal geometry around copper; the exception being **9a**, for which a τ-value of 0.7 and the Cu-ligand distances indicate a trigonal-bipyramidal geometry. As in **4a**-**6a**, the amine occupies the apical position in **10a**. As in **6b**, the alkoxide is found in that position in **8b**. In **11b**, pyridine occupies the apical position. Contrary to most of the structural deviations observed in the complexes studied here, a clear steric motivation exists in this case: placing the bridging alkoxide in the apical position, as in **6b** and **8b**, would lead for **11b** to strong steric interactions between the xylyl substituent and the bridging pyridylmethanol.

Polymerizations with **8b** and **11b** showed a notable induction period, while polymerizations with **9a** did not (Fig. 5). In this,

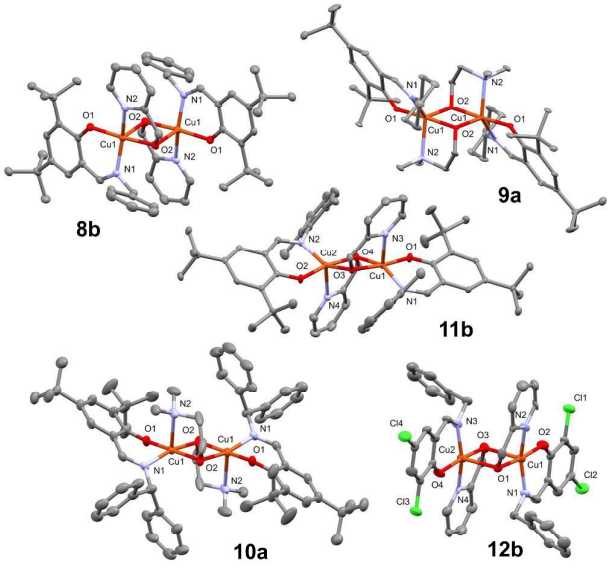

Figure 4. X-ray structures of **8b**, **9a**, **10a**, and **11b** and **12b**. Thermal displacements are shown at the 50% probability level. Hydrogen atoms and solvent (**8b**) were omitted for clarity. Only one of two independent molecules shown for **8b**.

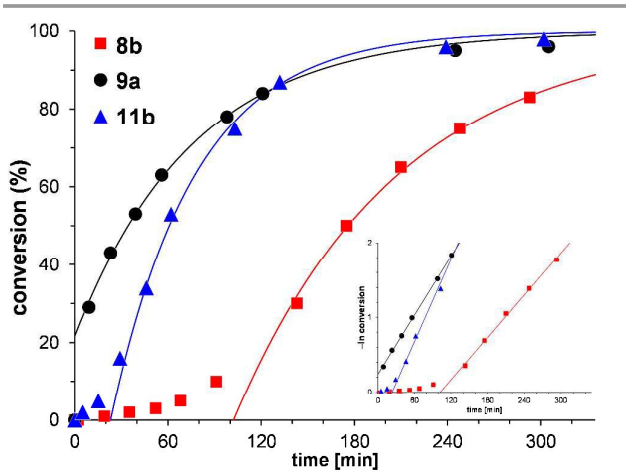

Figure 5 Conversion-time profiles for *rac*-lactide polymerization with **8b** (squares), **9a** (circles) and, **11b** (triangles). Conditions: C_6D_6, RT, 0.2 M lactide, 2 mM cat.. The inset shows the semi-logarithmic plot. Solid lines represent in both graphics theoretical conversions with the values obtained in linear regression analysis: **8b**: k_{app} = 0.57(2) h^{-1}, t_0 = 102 min, **9a**: k_{app} = 0. 0.78(1) h^{-1}, t_0 = –19 min, **11b**: k_{app} = 1.1(1) h^{-1}, t_0 = 23 min.

View Article Online
DOI: 10.1039/C8DT02140F

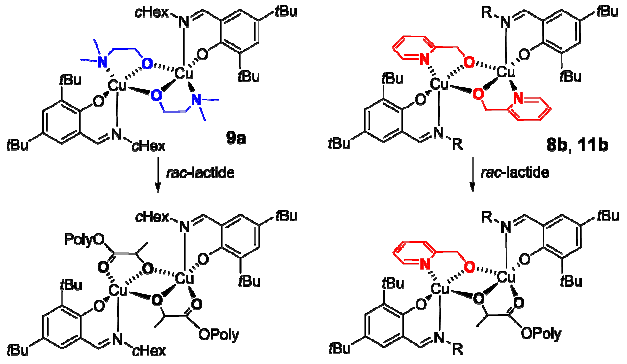

Scheme 7

iminophenoxide complexes resemble their iminopyrrolide analogues, where an induction period was associated with the pyridylmethoxide bridging ligand. All polymerizations went to completion in less than 5 h, although some catalyst decomposition was observed for **9a**. Polymer molecular weight control was significantly improved and PLA polydispersities were below 1.3 for all catalysts (Table 2). More important, the obtained molecular weights indicate that only one pyridylmethoxide ligand initiates chain growth in **8b** and **11b**, while both alkoxides initiate chain growth in **9a**. Iminophenoxide complexes thus follow the same mechanism observed for iminopyrrolide complexes and the active species in polymerizations with **8b** and **11b** is most likely a pyridylmethoxide-bridged dinuclear compound (Scheme 7). However, unlike iminopyrrolide complexes, neither **8b**, nor **11b** or **9a** with pyridylmethoxide added, showed any preference for isotactic polymerization and the obtained PLA was atactic (Table 2).

1,3-dichlorosalicylaldehyde-based ligands.

Increased σ-donation from the spectator ligand weakens the coordination of the bridging group. Since stereoselectivity correlated with the "rigidity" of the bridging ligand, increased σ-donation might thus be detrimental for stereocontrol. We investigated iminophenoxide ligands with *ortho*- and *para*-chloro substituents, to reduce σ-donation from the phenoxide ligand. Unfortunately, all attempts to prepare aminoethoxide or pyridylmethoxide complexes with ligands **L12**H-**L15**H yielded the homoleptic complexes **12c**-**15c** (Fig. S2), with the exception of the *N*-benzyl complex **12b**. The solid state structure of complex **12b** is very similar to that of **8b**. It is tempting to assign a shorter Cu-$O_{phenoxide}$ and Cu-$N_{pyridine}$ to a higher Lewis-acidity of the copper center, but comparison with all structural data from **6b**, **8b**, **11b**, and **12b** does not show a clear correlation between phenoxide ligand σ-donor ability and bond lengths. Unfortunately, complex **12b** is essentially inactive in polymerization; either due to decomposition or because monomer was unable to replace the bridging alkoxide. We were thus unable to determine the influence of σ-donation on isotacticity.

Conclusion

Heteroleptic copper complexes based on 4,6-di(*tert*-butyl)substituted iminophenoxide ligands are successful catalysts for the coordination-insertion polymerization of *rac*-lactide at room temperature. They produce PLA with good activities and high polymer molecular weight control. Their solid-state structures strongly resemble those of the analogous iminopyrrolide complexes and, based on polymer molecular weight data, they form the same dinuclear active species which retains an unreacted pyridylmethoxide ligand. Nevertheless, no stereocontrol was observed, which might be attributed to an increased σ-donation from the spectator ligand. Stereocontrol in dinuclear copper complexes of this type thus seems to require hitting the exact spot of sufficient rigidity/Lewis-acidity in the dinuclear complex to ensure stereocontrol, without encountering loss of activity.

Experimental

General considerations. All reactions were carried out using Schlenk or glove box techniques under nitrogen atmosphere. $Cu(OMe)_2$,[97] 4,6-di-tert-butylsalicyladehyde,[98] 1,3-dichlorosalicyladehyde,[98] **L2**H,[99] **L3**H,[100] **L8**H,[101] **L9**H,[101] **L10**H,[102] and **L11**H[103] were prepared according to literature. Solvents were dried by passage through activated aluminum oxide (MBraun SPS), de-oxygenated by repeated extraction with nitrogen, and stored over molecular sieves. C_6D_6 was dried over molecular sieves. *rac*-Lactide (98%) was purchased from Sigma–Aldrich, purified by 3x recrystallization from dry ethyl acetate and kept at –30 °C. All other chemicals were purchased from common commercial suppliers and used without further purification. ^{1}H and ^{13}C NMR spectra were acquired on Bruker Avance 300 and 400 spectrometers. Chemical shifts were referenced to the residual signals of the deuterated solvents ($CDCl_3$: ^{1}H: δ 7.26 ppm, ^{13}C: δ 77.16). Elemental analyses were performed by the Laboratoire d'analyse élémentaire (Université de Montréal). Molecular weight analyses were performed on a Waters 1525 gel permeation chromatograph equipped with three Phenomenex columns and a refractive index detector at 35 °C. THF was used as the eluent at a flow rate of 1.0 mL·min^{-1} and polystyrene standards (Sigma–Aldrich, 1.5 mg·mL^{-1}, prepared and filtered (0.2 mm) directly prior to injection) were used for calibration. Obtained molecular weights were corrected by a Mark-Houwink factor of 0.58.[104] All UV-Vis measurements were done in degassed and anhydrous toluene at RT in a sealed quartz cell on a Cary 500i UV-Vis-NIR Spectrophotometer. ^{1}H NMR spectra of paramagnetic Cu(II) compounds either provided peaks broadened to an extend that they were indistinguishable from the baseline or they showed one strongly broadened peak, the displacement of which was essentially invariant from the composition of the complex. NMR data is thus not provided for Cu(II) complexes.

2-((Benzylimino)methyl)phenol, L4H. A procedure from literature was modified as follows. Salicylaldehyde (1.0 g, 8.2 mmol) was dissolved in dry toluene (25 mL). $MgSO_4$ (5.0 g) , a

View Article Online
DOI: 10.1039/C8DT02140F

catalytic amount of Amberlyst 15 and benzylamine (0.88 g, 8.2 mmol) were added. The reaction was refluxed for 4 h. The yellow suspension was filtered and the solvent removed under vacuum. The residue was treated with hexane (20 mL), resulting in a light yellow oil. The oil was separated by decantation and dried under vacuum to give (1.69 g, 98%).

^{1}H NMR ($CDCl_3$, 400 MHz): δ 8.45 (s, 1H, (N=C)*H*), 7.40 – 7.23 (m, 7H, Ar), 6.97 (d, *J* = 8 Hz, 1H, Ar), 6.89 (td, *J* = 8, 1 Hz, 1H, Ar), 4.82 (s, 2H, CH_2).

2-((Cyclohexylimino)methyl)phenol, L5H. Analogous to **L4**H, from salicylaldehyde (1.0 g, 8.2 mmol), dry toluene (25 mL), 5g $MgSO_4$, a catalytic amount of Amberlyst 15, cyclohexylamine (0.81 g, 8.2 mmol) and refluxed for 4 hours to yield a light yellow oil (1.64g, 98%).

^{1}H NMR ($CDCl_3$, 400 MHz): δ 8.36 (s, 1H, (N=C)*H*), 7.29 (td, *J* = 8, 1 Hz, 1H, Ar), 7.23 (dd, *J* = 8, 1 Hz, 1H, Ar), 6.95 (d, *J* = 8 Hz, 1H, Ar), 6.86 (td, *J* = 8, 1 Hz, 1H, Ar), 3.24 (t, *J* = 10 Hz, 1H, NCH), 1.90 – 1.72 (m, 4H, CH_2), 1.72 – 1.48 (m, 3H, CH_2), 1.48 – 1.21 (m, 3H, CH_2).

2-((Diphenylmethylimino)methyl)phenol, L6H. Analogous to **L4**H, from salicylaldehyde (1.0 g, 8.2 mmol), dry toluene (25 mL), 5g $MgSO_4$, a catalytic amount of Amberlyst 15, diphenylmethylamine (1.5 g, 8.2 mmol) and refluxed for 4 hours to yield a light yellow oil (2.21 g, 94%).

^{1}H NMR ($CDCl_3$, 400 MHz): δ 8.48 (s, 1H, (N=C)H), 7.38 – 7.22 (m, 13H, Ar), 6.99 (d, *J* = 8 Hz, 1H, Ar), 6.89 (td, *J* = 8, 1 Hz, 1H, Ar), 5.63 (s, 1H, CH).

2-((2,6-Dimethylphenylimino)methyl)phenol, L7H. Analogous to **L4**H, from salicylaldehyde (1.0 g, 8.2 mmol), dry toluene (25 mL), 5g $MgSO_4$, a catalytic amount of Amberlyst 15, 2,6-xylylamine (1.0 g, 8.2 mmol) and refluxed for 4 hours to yield a light yellow oil (1.82 g, 98%).

^{1}H NMR ($CDCl_3$, 400 MHz): δ 13.10 (s, 1H, OH), 8.35 (s, 1H, (N=C)*H*), 7.46 – 7.38 (m, 1H, Ar), 7.36 (dd, *J* = 8, 1 Hz, 1H, Ar), 7.16 – 7.01 (m, 4H, Ar), 6.97 (td, *J* = 8, 1 Hz, 1H, Ar), 2.21 (d, *J* = 8 Hz, 6H, CH_3).

1,3-Dichloro-6-((benzylimino)methyl)phenol, L12H. Analogous to L4H, from 3,5-dichlorosalicylaldehyde (1.0 g, 8.2 mmol), dry toluene (25 mL), 5g $MgSO_4$, a catalytic amount of Amberlyst 15, benzylamine (0.88 g, 8.2 mmol) (1.5 g, 8.2 mmol) and refluxed for 4 hours to yield a light yellow oil which was purified by silica gel chromatography (10% EtOAc in hexane) (1.68 g, 73%).

^{1}H NMR ($CDCl_3$, 300 MHz): δ 8.33 (s, 1H, (N=C)*H*), 7.43 – 7.27 (m, 6H, Ar), 7.17 (d, *J* = 3 Hz, 1H, Ar), 4.84 (s, 2H, CH_2); ^{13}C{^{1}H} NMR ($CDCl_3$, 75 MHz): δ 163.9 ((N=)C), 157.1 (C-OH), 137.0 (ipso-Ph), 132.5 (Ar), 129.2 (Ar), 129.0 (o-Ph), 128.1 (m-Ph), 128.0 (Ar), 123.1 (Ar), 122.7 (Ar), 119.6 (Ar), 62.4 (CH_2). ESI-HRMS (m/z): $[M+H]^+$ ($C_{14}H_{12}Cl_2NO$) calcd 280.0290; found 280.0290.

1,3-dichloro-6-((cyclohexylimino)methyl)phenol, L13H. Analogous to L4H, from 3,5-Dichlorosalicylaldehyde (1.0 g, 8.2 mmol), dry toluene (25 mL), 5g $MgSO_4$, a catalytic amount of Amberlyst 15, cyclohexylamine (0.88 g, 8.2 mmol) (1.5 g, 8.2 mmol) and refluxed for 4 hours to yield a light yellow oil which was purified by silica gel chromatography (5% EtOAc in hexane) (1.71 g, 77%).

^{1}H NMR ($CDCl_3$, 300 MHz): δ 8.21 (s, 1H, (N=C)*H*), 7.40 (d, *J* = 3 Hz, 1H, o-Ph), 7.11 (d, *J* = 3 Hz, 1H, m-Ph), 3.37 (tt, *J* = 10, 3 Hz, 1H, NCH) 1.95 – 1.85 (m, 4H, CH_2), 1.73 – 1.21 (m, 6H); ^{13}C{^{1}H} NMR ($CDCl_3$, 75 MHz): δ 161.1 ((N=)C), 159.7 (C-OH), 132.6 (Ar), 129.0 (Ar), 124.0 (Ar), 121.3 (Ar), 118.7 (Ar), 65.6 (NCH), 34.0 (CH_2), 25.4 (CH_2), 24.2 (CH_2). ESI-HRMS (m/z): $[M+H]^+$ ($C_{13}H_{16}Cl_2NO$) calcd 272.0603; found 272.0614.

1,3-dichloro-6-((diphenylmethylimino)methyl)phenol, L14H. Analogous to L4H, from 3,5-Dichlorosalicylaldehyde (1.0 g, 8.2 mmol), dry toluene (25 mL), 5g $MgSO_4$, a catalytic amount of Amberlyst 15, diphenylmethylamine (0.88 g, 8.2 mmol) (1.5 g, 8.2 mmol) and refluxed for 4 hours to yield a light yellow oil which was purified by silica gel chromatography (5% EtOAc in hexane) (1.76g, 60%).

^{1}H NMR ($CDCl_3$, 300 MHz): δ 8.38 (s, 1H, (N=C)*H*), 7.42 (d, *J* = 3 Hz, 1H, o-Ph), 7.39 – 7.26 (m, 10H, Ar), 7.17 (d, *J* = 3 Hz, 1H, p-Ph), 5.69 (s, 1H, CH); ^{13}C{^{1}H} NMR ($CDCl_3$, 75 MHz): δ 163.5 ((N=)C), 156.5 (C-OH), 141.7 (Ar), 132.6 (ipso-Ph), 129.5 (Ar), 129.0 (o-Ph), 127.9 (Ar), 127.6 (m-Ph), 123.1 (Ar), 122.9 (Ar), 119.9 (Ar), 76.4 (CH). ESI-HRMS (m/z): $[M+H]^+$ ($C_{20}H_{16}Cl_2NO$) calcd 356.0603; found 356.0617.

1,3-dichloro-6-((2,6-dimethylphenylimino)methyl)phenol, L15H. Analogous to L4H, from 3,5-dichlorosalicylaldehyde (1.0 g, 8.2 mmol), dry toluene (25 mL), 5g $MgSO_4$, a catalytic amount of Amberlyst 15, 2,6-xylylamine (0.88 g, 8.2 mmol) (1.5 g, 8.2 mmol) and refluxed for 4 hours to yield a light yellow oil which was purified by silica gel chromatography (5% EtOAc in hexane) (1.93 g, 80%).

^{1}H NMR ($CDCl_3$, 300 MHz): δ 8.28 (s, 1H, (N=C)*H*), 7.50 (d, *J* = 3 Hz, 1H, o-Ph), 7.25 (d, *J* = 3 Hz, 1H, p-Ph), 7.15 – 7.01 (m, 3H, Ar), 2.20 (s, 6H, CH_3); ^{13}C{^{1}H} NMR ($CDCl_3$, 75 MHz): δ 165.3 ((N=)C), 156.21 (C-OH), 147.1 (Ar), 133.0 (Ar), 129.9 (Ar), 128.7 (Ar), 128.5 (Ar), 125.9 (Ar), 123.5 (Ar), 123.1 (Ar), 119.9 (Ar), 18.6 (CH_3). ESI-HRMS (m/z): $[M+H]^+$ ($C_{15}H_{14}Cl_2NO$) calcd 294.0452; found 294.0460.

[(L2)$_2$Cu$_2$(μ-O,κ$_N$-OC$_2$H$_4$NMe$_2$)$_2$], 2a. $Cu(OMe)_2$ (67 mg, 0.53 mmol) was suspended in toluene (3 mL). Dimethylaminoethanol (110 μl, 1.1 mmol) was added to the blue suspension and stirred for 45 min. A freshly prepared colourless solution of **L2**H (100 mg, 0.53 mmol) in toluene (2 mL) was added dropwise, resulting in a dark-green solution. The reaction was stirred 24 hours at RT, filtered to remove trace impurities and concentrated to 1/3 of the volume, Green crystals separated on standing, were separated by decantation and washed with ether (3×10 mL) (40 g, 22%).

UV-vis (toluene, $3.5\cdot10^{-6}$M) [λ_{max}, nm (ε, mol^{-1} cm^2)]: 305 (35000), 385 (5800), 657 (2200). Anal. Calcd for $C_{32}H_{48}Cu_2N_4O_4$: C, 56.53; H, 7.12; N, 8.24; Found: C, 56.17; H, 7.48; N, 8.27.

[(L3)Cu(μ-O,κ$_N$-OCH$_2$Py)], 3b. Analogous to **2a,** from $Cu(OMe)_2$ (59 mg, 0.47 mmol) in toluene (3 mL), 2-pyridinemethanol (91 μL, 0.94 mmol), **L3**H (100 mg, 0.47 mmol) in toluene (2 mL). Filtration and concentration (1/3 of the volume) of the green solution, decantation and washing with ether (3 x 10 mL) afforded 27 mg (15%) of green X-ray quality crystals.

UV-vis (toluene, $1.6\cdot10^{-5}$M) [λ_{max}, nm (ε, mol^{-1} cm^2)]: 294 (sh), 384 (580), 408 (400), 487 (270), 668 (180). Anal. Calcd for

View Article Online
DOI: 10.1039/C8DT02140F

$C_{20}H_{20}CuN_2O_2$: C, 63.47; H, 5.33; N, 8.54; Found: C, 63.53; H, 5.59; N, 8.50.

$(L4)_2Cu_2(\mu\text{-}O,\kappa_N\text{-}OC_2H_4NMe_2)_2$, 4a. Analogous to **2a,** from $Cu(OMe)_2$ (59 mg, 0.47 mmol) in toluene (3 mL), dimethylaminoethanol (95 µL, 0.94 mmol), **L4**H (100 mg, 0.47 mmol) in toluene (2 mL). Filtration and concentration (1/3 of the volume) of the green solution, decantation and washing with ether (3 x 10 mL) afforded 30 mg (18%) of green X-ray quality crystals.

UV-vis (toluene, $1.7\cdot10^{-5}$M) [λ_{max}, nm (ε, mol^{-1} cm^2)]: 303 (sh), 373 (9200), 472 (950), 664 (300). Anal. Calcd for $C_{36}H_{44}Cu_2N_4O_4$: C, 59.73; H, 6.13; N, 7.74; Found: C, 59.62; H, 6.52; N, 7.82.

$(L4)_2Cu$, 4c. Analogous to **2a**, without the addition of alcohol: $Cu(OMe)_2$ (30 mg, 0.24 mmol)) was suspended in toluene (3 mL). A freshly prepared solution of **L4**H (100 mg, 0.47 mmol) in toluene (2 mL) was added dropwise. The reaction was stirred for 24 h, filtered to remove trace impurities and concentrated to 1/3 of its volume. Brown crystals separated on standing and were isolated by decantation and washing with hexane (3 x 10 mL) to afford 61 mg (53%) of brown X-ray quality crystals. For the X-ray structure, see Fig. S2. Synthesis[92] and a polymorph[91] of this complex have been reported previously.

UV-vis (toluene, $2.1\cdot10^{-5}$M) [λ_{max}, nm (ε, mol^{-1} cm^2)]: 307 (sh), 373 (5000), 471 (sh), 644 (300). Anal. Calcd for $C_{28}H_{24}CuN_2O_2$: C, 69.48; H, 5.00; N, 5.79; Found: C, 69.52; H, 5.30; N, 5.49.

$(L5)_2Cu_2(\mu\text{-}O,\kappa_N\text{-}OC_2H_4NMe_2)_2$, 5a. Analogous to **2a,** from $Cu(OMe)_2$ (62 mg, 0.49 mmol) in toluene (3 mL), dimethylaminoethanol (98 µL, 0.98 mmol), **L5**H (100 mg, 0.49 mmol) in toluene (2 mL). Filtration and concentration (1/3 of the volume) of the green solution, decantation and washing with ether (3 x 10 mL) afforded 35 mg (20%) of green X-ray quality crystals. For the X-ray structure, see Fig. S2.

UV-vis (toluene, $8.7\cdot10^{-5}$M) [λ_{max}, nm (ε, mol^{-1} cm^2)]: 317 (sh), 370 (1700), 463 (200), 663 (50). Anal. Calcd for $C_{34}H_{52}Cu_2N_4O_4$: C, 57.69; H, 7.40; N, 7.91; Found: C, 57.30; H, 8.02 N, 7.81.

$(L5)_2Cu$, 5c. Analogous to **4c**, from $Cu(OMe)_2$ (31 mg, 0.25 mmol), toluene (3 mL), **L5**H (100 mg, 0.49 mmol) in toluene (2 mL), 59 mg (50%) of green X-ray quality crystals. For the X-ray structure, see Fig. S2. Synthesis[105] and structure[106] of this complex have been reported previously.

UV-vis (toluene, $2.1\cdot10^{-5}$M) [λ_{max}, nm (ε, mol^{-1} cm^2)]: 314 (8300), 373 (8700), 467 (sh), 652 (300). Anal. Calcd for $C_{26}H_{32}CuN_2O_2$: C, 66.71; H, 6.89; N, 5.98; Found: C, 67.00; H, 7.23; N, 5.98.

$(L6)Cu_2(\mu\text{-}O,\kappa_N\text{-}OC_2H_4NMe_2)_2$, 6a. Analogous to **2a,** from $Cu(OMe)_2$ (44 mg, 0.35 mmol) in toluene (3 mL), dimethylaminoethanol (70 µL, 0.70 mmol), **L6**H (100 mg, 0.35 mmol) in toluene (2 mL). Filtration and concentration (1/3 of the volume) of the green solution, decantation and washing with ether (3 x 10 mL) afforded 28 mg (18%) of green X-ray quality crystals.

UV-vis (toluene, $3.5\cdot10^{-5}$M) [λ_{max}, nm (ε, mol^{-1} cm^2)]: 315 (2300), 349 (sh), 374 (1800), 475 (100). Anal. Calcd for $C_{48}H_{52}Cu_2N_4O_4.1H_2O$: C, 64.48; H, 6.09; N, 6.27; Found: C, 64.11; H, 6.16; N, 6.25.

$(L6)_2Cu_2(\mu\text{-}O,\kappa_N\text{-}OCH_2Py)_2$, 6b. Analogous to **2a,** from $Cu(OMe)_2$ (44 mg, 0.35 mmol) in toluene (3 mL), 2-pyridinemethanol (67 µL, 0.70 mmol), **L6**H (100 mg, 0.35 mmol) in toluene (2 mL). Filtration and concentration (1/3 of the volume) of the green solution, decantation and washing with ether (3 x 10 mL) afforded 24 mg (15%) of green X-ray quality crystals.

UV-vis (toluene, $1\cdot10^{-5}$M) [λ_{max}, nm (ε, mol^{-1} cm^2)]: 318 (6000), 352 (sh), 373 (5000), 474 (300). Anal. Calcd for $C_{52}H_{44}Cu_2N_4O_4\cdot1/2C_4H_{10}O$: C, 68.05; H, 5.18; N, 5.88; Found: C, 67.58; H, 4.89; N, 6.29.

$(L6)_2Cu$, 6c. Analogous to **4c**, from $Cu(OMe)_2$ (21 mg, 0.17 mmol) in toluene (3 mL), **L6**H (100 mg, 0.35 mmol) in toluene (2 mL), 53 mg (49%) of brown X-ray quality crystals.

UV-vis (toluene, $3.3\cdot10^{-5}$M) [λ_{max}, nm (ε, mol^{-1} cm^2)]: 327 (sh), 388 (2700), 671 (200). Anal. Calcd for $C_{40}H_{32}CuN_2O_2\cdot1/2C_7H_8$: C, 76.57; H, 5.32; N, 4.11; Found: C, 76.67; H, 5.78; N, 4.32. For the X-ray structure, see Fig. S2. Synthesis[107] and a polymorph[108] of this complex have been reported previously.

$(L7)_2Cu$, 7c. Analogous to **4c,** from $Cu(OMe)_2$ (28 mg, 0.22 mmol) in toluene (3 mL), **L7**H (100 mg, 0.44 mmol) in toluene (2 mL). Filtration and concentration (1/3 of the volume) of the brown solution, decantation and washing with hexane (3 x 10 mL) afforded 56 mg (50%) of brown X-ray quality crystals.

UV-vis (toluene, $2.2\cdot10^{-5}$M) [λ_{max}, nm (ε, mol^{-1} cm^2)]: 333 (sh), 411 (3200), 512 (sh), 683 (240). Anal. Calcd for $C_{30}H_{28}CuN_2O_2$: C, 70.36; H, 5.51; N, 5.47; Found: C, 70.35; H, 5.69; N, 5.54. For the X-ray structure, see Fig. S2. Synthesis[105] of this complex have been reported previously.

$(L8)_2Cu_2(\mu\text{-}O,\kappa_N\text{-}OCH_2Py)_2$, 8b. Analogous to **2a,** from $Cu(OMe)_2$ (39 mg, 0.31 mmol) in toluene (3 mL), 2-pyridinemethanol (60 µL, 0.62 mmol), **L8**H (100 mg, 0.31 mmol) in toluene (2 mL). Filtration and concentration (1/3 of the volume) of the green solution, decantation and washing with ether (3 x 10 mL) afforded 26 mg (17%) of green X-ray quality crystals.

UV-vis (toluene, $1.14\cdot10^{-5}$M) [λ_{max}, nm (ε, mol^{-1} cm^2)]: 332 (6200), 400 (sh), 503 (300), 666 (200). Anal. Calcd for $C_{56}H_{68}Cu_2N_4O_4$: C, 68.06; H, 6.94; N, 5.67; Found: C, 68.54; H, 7.36; N, 5.41.

$(L9)_2Cu_2(\kappa_N\text{-}OC_2H_4NMe_2)_2$, 9a. Analogous to **2a,** from $Cu(OMe)_2$ (40 mg, 0.32 mmol) in toluene (3 mL), dimethylaminoethanol (64 µL, 0.64 mmol), **L9**H (100 mg, 0.32 mmol) in toluene (2 mL). Filtration and concentration (1/3 of the volume) of the green solution, decantation and washing with ether (3 x 10 mL) afforded 27 mg (18%) of green X-ray quality crystals.

UV-vis (toluene, $1.4\cdot10^{-5}$M) [λ_{max}, nm (ε, mol^{-1} cm^2)]: 324 (8800), 390 (6800), 479 (500). Anal. Calcd for $C_{50}H_{84}Cu_2N_4O_4$: C, 64.41; H, 9.08; N, 6.01; Found: C, 64.63; H, 9.87; N, 5.90.

$(L10)_2Cu_2(\mu\text{-}O,\kappa_N\text{-}OC_2H_4NMe_2)_2$, 10a. Analogous to **2a,** from $Cu(OMe)_2$ (40 mg, 0.25 mmol) in toluene (3 mL), dimethylaminoethanol (63 µL, 0.50 mmol), **L10**H (100 mg, 0.25 mmol) in toluene (2 mL). Filtration and concentration (1/3 of the volume) of the green solution afforded just a few green X-ray quality crystals.

$(L11)_2Cu_2(\mu\text{-}O,\kappa_N\text{-}OCH_2Py)_2$, 11b. Analogous to **2a,** from $Cu(OMe)_2$ (38 mg, 0.30 mmol) in toluene (3 mL), 2-

View Article Online
DOI: 10.1039/C8DT02140F

pyridinemethanol (57 µL, 0.60 mmol), **L11**H (100 mg, 0.30 mmol) in toluene (2 mL). Filtration and concentration (1/3 of the volume) of the green solution, decantation and washing with ether (3 x 10 mL) afforded 29 mg (19%) of green X-ray quality crystals.

UV-vis (toluene, $3.3\cdot10^{-5}$M) [λ_{max}, nm (ε, mol^{-1} cm^2)]: 334 (sh); 402 (15000), 505 (1200), 662 (300). Anal. Calcd for $C_{58}H_{72}Cu_2N_4O_4$: C, 68.54; H, 7.14; N, 5.51; Found: C, 68.41; H, 7.86; N, 5.24.

(L12)$_2$Cu$_2$(µ-O,κ_N-OCH$_2$Py)$_2$, 12b. Analogous to **2a,** from $Cu(OMe)_2$ (45 mg, 0.36 mmol) in toluene (3 mL), 2-pyridinemethanol (70 µL, 0.72 mmol), **L12**H (100 mg, 0.36 mmol) in toluene (2 mL). Filtration and concentration (1/3 of the volume) of the green solution, decantation and washing with ether (3 x 10 mL) afforded 18 mg (11%) of green X-ray quality crystals.

UV-vis (toluene, $1.1\cdot10^{-5}$M) [λ_{max}, nm (ε, mol^{-1} cm^2)]: 386 (9000), 484 (sh). Anal. Calcd for $C_{40}H_{32}Cl_4Cu_2N_4O_4$: C, 53.29; H, 3.58; N, 6.21; Found: C, 53.57; H, 3.74; N, 6.26.

(L12)$_2$Cu, 12c. Analogous to **2a,** from $Cu(OMe)_2$ (23 mg, 018 mmol) in toluene (3 mL), **L12**H (100 mg, 0.36 mmol) in toluene (2 mL). Filtration and concentration (1/3 of the volume) of the brown solution, decantation and washing with hexane (3 x 10 mL) afforded 60 mg (54%) of brown X-ray quality crystals. For the X-ray structure, see Fig. S2. Elemental analysis differs notably from theoretical values, indicating notable amounts of impurities. No further attempt of purification was attempted.

UV-vis (toluene, $1.1\cdot10^{-5}$M) [λ_{max}, nm (ε, mol^{-1} cm^2)]: 309 (sh), 384 (6800), 470 (sh), 658 (270). Anal. Calcd for $C_{28}H_{20}Cl_4CuN_2O_2$: C, 54.08; H, 3.24; N, 4.51; Found: C, 50.50; H, 4.94; N, 6.26.

(L13)$_2$Cu, 13c. Analogous to **2a,** from $Cu(OMe)_2$ (24 mg, 0.19 mmol) in toluene (3 mL), **L13**H (100 mg, 0.37 mmol) in toluene (2 mL). Filtration and concentration (1/3 of the volume) of the brown solution, decantation and washing with hexane (3 x 10 mL) afforded 68 mg (59%) of brown X-ray quality crystals. For the X-ray structure, see Fig. S2. Synthesis of this complex have been reported previously.[109]

UV-vis (toluene, $1.4\cdot10^{-5}$M) [λ_{max}, nm (ε, mol^{-1} cm^2)]: 301 (sh), 379 (7000), 486 (sh), 671 (300). Anal. Calcd for $C_{26}H_{28}Cl_4CuN_2O_2$: C, 51.54; H, 4.66; N, 4.62; Found: C, 51.81; H, 4.84; N, 4.65.

(L12)$_2$Cu, 14c. Analogous to **5,** from $Cu(OMe)_2$ (18 mg, 0.14 mmol) in toluene (3 mL), **L14**H (100 mg, 0.28 mmol) in toluene (2 mL). Filtration and concentration (1/3 of the volume) of the brown solution, decantation and washing with hexane (3 x 10 mL) afforded 62 mg (57%) of brown X-ray quality crystals. For the X-ray structure, see Fig. S2.

UV-vis (toluene, $1.1\cdot10^{-5}$M) [λ_{max}, nm (ε, mol^{-1} cm^2)]: 309 (sh), 381 (6500), 485 (sh), 679 (370). Anal. Calcd for $C_{40}H_{28}Cl_4CuN_2O_2$: C, 62.07; H, 3.65; N, 3.62; Found: C, 61.75; H, 3.88; N, 3.68.

(L15)$_2$Cu, 15c. Analogous to **2a,** from $Cu(OMe)_2$ (21 mg, 0.17 mmol) in toluene (3 mL), **L15**H (100 mg, 0.34 mmol) in toluene (2 mL). Filtration and concentration (1/3 of the volume) of the the green solution afforded just a few green X-ray quality crystals. For the X-ray structure, see Fig. S2.

View Article Online
DOI: 10.1039/C8DT02140F

$(C_7H_6O_2)_2Cu_2(\mu\text{-}O,\kappa_N\text{-}OC_2H_4NMe_2)_2$, 16a. Analogous to **2a,** from $Cu(OMe)_2$ (103 mg, 0.82 mmol) in toluene (3 mL), dimethylaminoethanol (165 µl, 1.64 mmol), salicylaldehyde (100 mg, 0.82 mmol) in toluene (2 mL). Filtration and concentration (1/3 of the volume) of the green solution, decantation and washing with ether (3 x 10 mL) afforded 32 mg (14%) of green X-ray quality crystals.

UV-vis (toluene, $1.9\cdot10^{-5}$ M) [λ_{max}, nm (ε, mol^{-1} cm^2)]: 292 (5000), 319 (4500), 374 (3500), 474 (sh), 675 (350). Anal. Calcd for $C_{22}H_{30}Cu_2N_2O_6$: C, 48.43; H, 5.54; N, 5.13; Found: C, 48.15; H, 5.66; N, 5.13.

$(C_7H_6O_2)_2Cu_2(\mu\text{-}O,\kappa_N\text{-}OCH_2Py)_2$, 16b. Analogous to **2a,** from $Cu(OMe)_2$ (103 mg, 0.82 mmol) in toluene (3 mL), 2-pyridinemethanol (157 µL, 1.64 mmol), salicylaldehyde (100 mg, 0.82 mmol) in toluene (2 mL). Filtration and concentration (1/3 of the volume) of the green solution, decantation and washing with ether (3 x 10 mL) afforded 43 mg (18%) of green X-ray quality crystals.

UV-vis (toluene, $1.1\cdot10^{-4}$M) [λ_{max}, nm (ε, mol^{-1} cm^2)]: 293 (3000), 330 (2000), 372 (1500), 473 (400), 693 (120). Anal. Calcd for $C_{26}H_{22}Cu_2N_2O_6$: C, 53.33; H, 3.79; N, 4.78; Found: C, 53.73; H, 4.17; N, 5.13.

***rac*-Lactide polymerization**. For polymerizations at room temperature in solution, a solution of *rac*-lactide (28 mg, 0.20 mmol) in C_6D_6 was prepared in a J-Young tube inside the glovebox. If required, external alcohol was added as a stock solution in C_6D_6. The desired catalyst (2 µmol, appr. 100 µL of an appr. 20 mM stock solution in C_6D_6) was added and the solution completed to 1 mL total volume. Bulk polymerizations were conducted in a pressure tube which was prepared inside the glovebox with the addition of stock solution of the desired catalyst in C_6D_6, solid *rac*-lactide and benzyl alcohol (stock solution of 20 mM in C_6D_6). The pressure tube was sealed and immersed for 24 h in an oil bath pre-heated to 130 °C. In both cases, polymerization reactions were quenched with 5 equiv of acetic acid (relative to catalyst) in $CDCl_3$ (5 mM). After determination of conversion and isotacticity, the solvent was evaporated and the polymer stored at –80 °C until GPC analysis.

X-ray diffraction studies. Single crystals were obtained described above. Diffraction data was collected either on a Bruker Venture METALJET diffractometer (Ga Kα radiation) or

Table 4. Details of X-ray Diffraction Studies

	2a	4a	5a	6a	9a	10a	16a
Formula	$C_{32}H_{48}Cu_2N_4O_4$	$C_{36}H_{44}Cu_2N_4O_4$	$C_{34}H_{52}Cu_2N_4O_4$	$C_{48}H_{52}Cu_2N_4O_4$	$C_{50}H_{84}Cu_2N_4O_4$	$C_{64}H_{84}Cu_2N_4O_4$	$C_{22}H_{30}Cu_2N_2O_6$
M_w (g/mol); $d_{calcd.}$ (g/cm^3)	679.8; 1.42	723.8; 1.45	707.9; 1.37	876.0; 1.41	932.3; 1.26	1100.4; 1.21	545.6; 1.52
T (K); F(000)	100; 716	100; 756	125; 634	100; 916	100; 2008	150; 586	100; 1128
Crystal System	Monoclinic	Monoclinic	Triclinic	Monoclinic	Monoclinic	Triclinic	Monoclinic
Space Group	$P2_1/c$	$P2_1/c$	$P(-1)$	$P2_1/n$	$C2/c$	$P(-1)$	$C2/c$
Unit Cell: a (Å)	10.2124(4)	9.4481(2)	10.494(2)	9.86980(10)	25.7609(11)	10.9595(5)	20.7678(3)
b (Å)	13.4671(6)	15.9169(4)	11.150(2)	14.7540(2)	9.3613(4)	11.4816(5)	6.11830(10)
c (Å)	11.5479(5)	11.5813(3)	15.860(3)	14.2160(2)	21.0180(9)	12.5663(5)	18.9079(3)
α (°)	90	90	90.01(3)	90	90	82.603(2)	90
β (°)	90.5560(10)	107.1780(10)	106.50(3)	92.1850(10)	104.466(2)	88.935(2)	97.71
γ (°)	90	90	104.32(3)	90	90	74.196(2)	90
V (Å^3); Z	1588.12(12); 2	1663.96(7); 2	1719.2(7); 2	2068.61(5); 2	4907.9(4); 4	1508.59(11); 1	2380.76(6); 4
μ (mm^{-1})	1.984	1.937	6.892	1.663	1.418	4.049	2.538
θ (°); completeness	3.3-72.0; 0.98	5.6 -72.0; 1	2.5-58.3; 0.96	5.4-72.1; 1	5.3-72.0; 0.99	3.1-60.7; 1.0	8.6-71.9; 0.98
collected reflections; R_σ	30005; 0.010	40807; 0.019	74452; 0.062	27872; 0.016	62412; 0.029	43024; 0.036	22853; 0.010
unique reflections; R_{int}	3074; 0.022	3260; 0.045	7348; 0.114	4058; 0.028	4796; 0.068	6935; 0.059	2304; 0.022
R1(F) ($I > 2\sigma(I)$)	0.027	0.032	0.107	0.033	0.061	0.063	0.023
wR(F^2) (all data)	0.074	0.094	0.329	0.092	0.166	0.169	0.063
GoF(F^2)	1.083	1.091	1.055	1.063	1.055	1.052	1.061
Residual electron density	0.36; –0.31	0.43; –0.35	2.23; –1.94	0.69; – 0.38	2.54; –1.18	1.58; –0.50	0.34; –0.29

View Article Online
DOI: 10.1039/C8DT02140F

Table 4 continued. Details of X-ray Diffraction Studies

	3b	6b	8b	11b	12b	16b
Formula	$C_{26}H_{27}CuN_3O_3$	$C_{52}H_{44}Cu_2N_4O_4$	$C_{63}H_{76}Cu_2N_4O_4$	$C_{72}H_{88}Cu_2N_4O_4$	$C_{40}H_{32}Cl_4Cu_2N_4O_4$	$C_{26}H_{22}Cu_2N_2O_6$
M_w (g/mol); $d_{calcd.}$ (g/cm^3)	493.04; 1.432	915.99; 1.462	1080.35; 1.307	1200.54; 1.246	901.57; 1.555	585.53; 1.210
T (K); F(000)	100; 1028	100; 948	100; 1144	100; 1276	150; 1832	100; 596
Crystal System	Monoclinic	Monoclinic	Triclinic	Monoclinic	Monoclinic	Monoclinic
Space Group	$P2_1/c$	$P2_1/n$	$P(-1)$	$P2_1$	$P2_1/n$	$P2_1/n$
Unit Cell: a (Å)	11.2111(3)	9.9716(3)	11.8306(4)	11.2710(5)	8.0732(5)	14.8060(2)
b (Å)	10.0858(3)	17.7646(5)	13.9522(5)	25.1487(10)	19.5258(11)	6.79250(10)
c (Å)	20.3125(6)	11.7580(3)	17.0501(6)	11.9113(5)	24.4945(14)	17.3010(3)
α (°)	90	90	102.745(2)	90	90	90
β (°)	95.2760(10)	92.5350(10)	90.632(2)	108.617(2)	94.265(3)	112.5270(10)
γ (°)	90	90	90.424(2)	90	90	90
V (Å^3); Z	2287.06(11); 4	2080.79(10); 2	2744.69(17); 2	3199.6(2); 2	3850.5(4); 4	1607.20(4); 2
μ (mm^{-1})	1.619	1.687	1.353	1.211	7.896	1.924
θ (°); completeness	3.96-71.99; 0.97	4.98-72.10; 0.99	3.72-71.79; 0.97	4.29-72.00; 0.96	2.52-60.66; 0.99	3.23-72.00; 0.99
collected reflections; R_σ	30049; 0.033	27977; 0.015	98116; 0.041	43734; 0.019	98818; 0.034	21072; 0.016
unique reflections; R_{int}	4360; 0.057	4065; 0.026	10437; 0.120	12091; 0.022	8870; 0.093	3146; 0.026
R1(F) ($I > 2\sigma(I)$)	0.033	0.032	0.060	0.026	0.033	0.032
wR(F^2) (all data)	0.092	0.087	0.166	0.071	0.164	0.090
GoF(F^2)	1.039	1.039	1.063	1.036	1.162	1.098
Residual electron density	0.38; –0.46	0.39; –0.33	1.31; –0.66	0.34; –0.29	0.66; – 0.61	0.90; – 0.30

a Bruker APEXII (Cu microsource/Quazar MX) with the application of the APEX software package, of SAINT for data reduction and of SADABS for absorption correction. Dual-space refinement (SHELXT) was used to solve structures. All non-hydrogen atoms were refined anisotropic by full matrix-least-squares on F^2 while hydrogen atoms were refined with fixed isotropic U by the application of a riding model (SHELXL97). Additional experimental data can be found in tables 4 and S1, and in the supporting information (CIF).

Conflicts of interest

There are no conflicts to declare.

Acknowledgements

Funding was supplied by the NSERC discovery program (RGPIN-2016-04953) and the Centre for Green Chemistry and Catalysis (FQRNT). We thank Marie-Christine Tang, Louiza Mahrouche and Alexandra Furtos for support with MALDI-MS and Francine Bélanger for support with X-ray crystallography.

Notes and references

1. V. Nagarajan, A. K. Mohanty and M. Misra, *ACS Sustainable Chem. Eng.*, 2016, **4**, 2899-2916.
2. E. Castro-Aguirre, F. Iñiguez-Franco, H. Samsudin, X. Fang and R. Auras, *Advanced drug delivery reviews*, 2016, **107**, 333-366.
3. S. Slomkowski, S. Penczek and A. Duda, *Polymers for Advanced Technologies*, 2014, **25**, 436-447.
4. M. Singhvi and D. Gokhale, *RSC Adv.*, 2013, **3**, 13558-13568.
5. T. A. Hottle, M. M. Bilec and A. E. Landis, *Polymer degradation and stability*, 2013, **2013 v.98 no.9**, pp. 1898-1907.
6. S. Inkinen, M. Hakkarainen, A.-C. Albertsson and A. Södergård, *Biomacromolecules*, 2011, **12**, 523-532.
7. J. Ahmed and S. K. Varshney, *Int. J. Food Prop.*, 2011, **14**, 37-58.
8. J. A. Vijayakumar, R.; Viruthagiri, T. , *Chem. Bio-chem. Eng. Q.*, 2008, **2**, 245-264.
9. Y. Tokiwa and B. P. Calabia, *Can. J. Chem.*, 2008, **86**, 548-555.
10. R. E. Drumright, P. R. Gruber and D. E. Henton, *Advanced Materials*, 2000, **12**, 1841-1846.

View Article Online
DOI: 10.1039/C8DT02140F

11. E. T. H. Vink, K. R. Rábago, D. A. Glassner, B. Springs, R. P. O'Connor, J. Kolstad and P. R. Gruber, *Macromolecular Bioscience*, 2004, **4**, 551-564.
12. S. Paul, Y. Zhu, C. Romain, R. Brooks, P. K. Saini and C. K. Williams, *Chem. Commun. (Cambridge, U. K.)*, 2015, **51**, 6459-6479.
13. I. d. S. Vieira and S. Herres-Pawlis, *European Journal of Inorganic Chemistry*, 2012, **2012**, 765-774.
14. S. Dutta, W.-C. Hung, B.-H. Huang and C.-C. Lin, in *Synthetic Biodegradable Polymers*, eds. B. Rieger, A. Künkel, G. W. Coates, R. Reichardt, E. Dinjus and T. A. Zevaco, Springer Berlin Heidelberg, Berlin, Heidelberg, 2012, DOI: 10.1007/12_2011_156, pp. 219-283.
15. P. J. Dijkstra, H. Du and J. Feijen, *Polym. Chem.*, 2011, **2**, 520-527.
16. J.-C. Buffet and J. Okuda, *Polym. Chem.*, 2011, **2**, 2758-2763.
17. C. M. Thomas, *Chem. Soc. Rev.*, 2010, **39**, 165.
18. M. J. Stanford and A. P. Dove, *Chemical Society Reviews*, 2010, **39**, 486-494.
19. C. K. Williams and M. A. Hillmyer, *Polymer Reviews*, 2008, **48**, 1-10.
20. N. Ajellal, J.-F. Carpentier, C. Guillaume, S. M. Guillaume, M. Helou, V. Poirier, Y. Sarazin and A. Trifonov, *Dalton Trans.*, 2010, **39**, 8363.
21. R. H. Platel, L. M. Hodgson and C. K. Williams, *Polym. Rev.*, 2008, **48**, 11 - 63.
22. J. Wu, T.-L. Yu, C.-T. Chen and C.-C. Lin, *Coord. Chem. Rev.*, 2006, **250**, 602-626.
23. O. Dechy-Cabaret, B. Martin-Vaca and D. Bourissou, *Chem. Rev.*, 2004, **104**, 6147-6176.
24. B. J. O'Keefe, M. A. Hillmyer and W. B. Tolman, *J. Chem. Soc., Dalton Trans.*, 2001, DOI: 10.1039/b104197p, 2215-2224.
25. M. H. Chisholm and Z. Zhou, *Journal of Materials Chemistry*, 2004, **14**, 3081-3092.
26. Z. Zhong, P. J. Dijkstra and J. Feijen, *J. Biomater. Sci., Polym. Ed.*, 2004, **15**, 929-946.
27. B. H. Huang, S. Dutta and C. C. Lin, in *Comprehensive Inorganic Chemistry II (Second Edition)*, ed. J. R. Poeppelmeier, Elsevier, Amsterdam, 2013, DOI: http://dx.doi.org/10.1016/B978-0-08-097774-4.00146-7, pp. 1217-1249.
28. C. A. Wheaton and P. G. Hayes, *Comments Inorg. Chem.*, 2011, **32**, 127-162.
29. C. A. Wheaton, P. G. Hayes and B. J. Ireland, *Dalton Transactions*, 2009, DOI: 10.1039/B819107G, 4832-4846.
30. A. K. Sutar, T. Maharana, S. Dutta, C.-T. Chen and C.-C. Lin, *Chem. Soc. Rev.*, 2010, **39**, 1724-1746.
31. E. Le Roux, *Coord. Chem. Rev.*, 2016, **306**, 65-85.
32. A. Sauer, A. Kapelski, C. Fliedel, S. Dagorne, M. Kol and J. Okuda, *Dalton Trans.*, 2013, **42**, 9007-9023.
33. J. P. MacDonald and M. P. Shaver, in *Green Polymer Chemistry: Biobased Materials and Biocatalysis*, American Chemical Society, 2015, vol. 1192, ch. 10, pp. 147-167.
34. R. Jianming, X. Anguo, W. Hongwei and Y. Hailin, *Designed Monomers and Polymers*, 2014, **17**, 345-355.
35. S. Dagorne, M. Normand, E. Kirillov and J.-F. Carpentier, *Coord. Chem. Rev.*, 2013, **257**, 1869-1886.
36. S. F. Dagorne, C.; de Frémont, P., in *In Encyclopedia of Inorganic and Bioinorganic Chemistry*, John Wiley & Sons, Ltd., 2011, DOI: doi:10.1002/9781119951438.eibc2416.
37. S. Dagorne and C. Fliedel, in *Modern Organoaluminum Reagents: Preparation, Structure, Reactivity and Use*, eds. S. Woodward and S. Dagorne, Springer Berlin Heidelberg, Berlin, Heidelberg, 2013, DOI: 10.1007/3418_2012_35, pp. 125-171.
38. A. Amgoune, M. Thomas Christophe and J.-F. Carpentier, *Journal*, 2007, **79**, 2013.
39. M. Cheng, A. B. Attygalle, E. B. Lobkovsky and G. W. Coates, *J. Am. Chem. Soc.*, 1999, **121**, 11583-11584.
40. T.-Q. Xu, G.-W. Yang, C. Liu and X.-B. Lu, *Macromolecules*, 2017, **50**, 515-522.
41. D. Myers, A. J. P. White, C. M. Forsyth, M. Bown and C. K. Williams, *Angew. Chem., Int. Ed.*, 2017, **56**, 5277-5282.
42. J. Bhattacharjee, A. Harinath, H. P. Nayek, A. Sarkar and T. K. Panda, *Chem.-Eur. J.*, 2017, **23**, 9319-9331.
43. Y. Sun, J. Xiong, Z. Dai, X. Pan, N. Tang and J. Wu, *Inorg. Chem.*, 2016, **55**, 136-143.
44. T. Rosen, Y. Popowski, I. Goldberg and M. Kol, *Chem.-Eur. J.*, 2016, **22**, 11533-11536.
45. P. McKeown, M. G. Davidson, G. Kociok-Kohn and M. D. Jones, *Chem. Commun. (Cambridge, U. K.)*, 2016, **52**, 10431-10434.
46. V. Balasanthiran, C. Chatterjee, M. H. Chisholm, N. D. Harrold, T. V. RajanBabu and G. A. Warren, *J. Am. Chem. Soc.*, 2015, **137**, 1786-1789.
47. Z. Mou, B. Liu, M. Wang, H. Xie, P. Li, L. Li, S. Li and D. Cui, *Chem. Commun. (Cambridge, U. K.)*, 2014, **50**, 11411-11414.
48. C. Bakewell, A. J. P. White, N. J. Long and C. K. Williams, *Angew. Chem., Int. Ed.*, 2014, **53**, 9226-9230.
49. D. C. Aluthge, B. O. Patrick and P. Mehrkhodavandi, *Chem. Commun. (Cambridge, U. K.)*, 2013, **49**, 4295-4297.
50. H. R. Kricheldorf and D.-O. Damrau, *J. Macromol. Sci., Part A: Pure Appl.Chem.*, 1998, **35**, 1875-1887.
51. B. B. Idage, S. B. Idage, A. S. Kasegaonkar and R. V. Jadhav, *Mater. Sci. Eng., B*, 2010, **168**, 193-198.
52. B. Rajashekhar and D. Chakraborty, *Polym. Bull.*, 2014, **71**, 2185-2203.
53. P. Daneshmand and F. Schaper, *Dalton Trans.*, 2015, **44**, 20449–20458.
54. A. Rathore, H. Kaur and R. Luque, *Journal of Polymer Research*, 2017, **25**, 2.
55. A. John, V. Katiyar, K. Pang, M. M. Shaikh, H. Nanavati and P. Ghosh, *Polyhedron*, 2007, **26**, 4033-4044.
56. L. Ding, W. Jin, Z. Chu, L. Chen, X. Lü, G. Yuan, J. Song, D. Fan and F. Bao, *Inorg. Chem. Commun.*, 2011, **14**, 1274-1278.
57. W.-J. Jin, L.-Q. Ding, Z. Chu, L.-L. Chen, X.-Q. Lü, X.-Y. Zheng, J.-R. Song and D.-D. Fan, *J. Molec. Catal. A: Chem.*, 2011, **337**, 25-32.
58. G. Xiao, B. Yan, R. Ma, W. J. Jin, X. Q. Lu, L. Q. Ding, C. Zeng, L. L. Chen and F. Bao, *Polym. Chem.*, 2011, **2**, 659-664.
59. A. Routaray, S. Mantri, N. Nath, A. K. Sutar and T. Maharana, *Polyhedron*, 2016, **119**, 335-341.
60. M. J. L. Tschan, J. Guo, S. K. Raman, E. Brule, T. Roisnel, M.-N. Rager, R. Legay, G. Durieux, B. Rigaud and C. M. Thomas, *Dalton Trans.*, 2014, **43**, 4550-4564.
61. S. Shin, S. Nayab and H. Lee, *Polyhedron*, 2018, **141**, 309-321.
62. J. Zhang, B. Wang, L. Wang, J. Sun, Y. Zhang, Z. Cao and Z. Wu, *Appl. Organomet. Chem.*, 2018, **32**, e4077.
63. B. J. O'Keefe, S. M. Monnier, M. A. Hillmyer and W. B. Tolman, *J. Am. Chem. Soc.*, 2001, **123**, 339-340.
64. V. C. Gibson, E. L. Marshall, D. Navarro-Llobet, A. J. P. White and D. J. Williams, *J. Chem. Soc., Dalton Trans.*, 2002, DOI: 10.1039/B209703F, 4321-4322.
65. D. S. McGuinness, E. L. Marshall, V. C. Gibson and J. W. Steed, *J. Polym. Sci., Part A: Polym. Chem.*, 2003, **41**, 3798-3803.
66. A. B. Biernesser, B. Li and J. A. Byers, *J. Am. Chem. Soc.*, 2013, **135**, 16553-16560.
67. A. Keuchguerian, B. Mougang-Soume, F. Schaper and D. Zargarian, *Can. J. Chem.*, 2015, **93**, 594–601.

View Article Online
DOI: 10.1039/C8DT02140F

68. L. A. Brown, F. S. Wekesa, D. K. Unruh, M. Findlater and B. K. Long, *J. Polym. Sci., Part A: Polym. Chem.*, 2017, **55**, 2824-2830.
69. C. M. Manna, A. Kaur, L. M. Yablon, F. Haeffner, B. Li and J. A. Byers, *J. Am. Chem. Soc.*, 2015, **137**, 14232-14235.
70. A. B. Biernesser, K. R. Delle Chiaie, J. B. Curley and J. A. Byers, *Angew. Chem., Int. Ed.*, 2016, **55**, 5251-5254.
71. R. Duan, C. Hu, X. Li, X. Pang, Z. Sun, X. Chen and X. Wang, *Macromolecules*, 2017, **50**, 9188-9195.
72. J. Sun, W. Shi, D. Chen and C. Liang, *J. Appl. Polym. Sci.*, 2002, **86**, 3312-3315.
73. R. R. Gowda and D. Chakraborty, *J. Molec. Catal. A: Chem.*, 2011, **349**, 86-93.
74. D. Appavoo, B. Omondi, I. A. Guzei, J. L. van Wyk, O. Zinyemba and J. Darkwa, *Polyhedron*, 2014, **69**, 55-60.
75. S. Bhunora, J. Mugo, A. Bhaw-Luximon, S. Mapolie, J. Van Wyk, J. Darkwa and E. Nordlander, *Appl. Organomet. Chem.*, 2011, **25**, 133-145.
76. C.-Y. Li, S.-J. Hsu, C.-l. Lin, C.-Y. Tsai, J.-H. Wang, B.-T. Ko, C.-H. Lin and H.-Y. Huang, *J. Polym. Sci., Part A: Polym. Chem.*, 2013, **51**, 3840-3849.
77. L.-L. Chen, L.-Q. Ding, C. Zeng, Y. Long, X.-Q. Lü, J.-R. Song, D.-D. Fan and W.-J. Jin, *Appl. Organomet. Chem.*, 2011, **25**, 310-316.
78. A. Routaray, N. Nath, T. Maharana and A. k. Sutar, *J. Macromol. Sci., Part A: Pure Appl.Chem.*, 2015, **52**, 444-453.
79. T. J. J. Whitehorne and F. Schaper, *Chem. Commun. (Cambridge, U. K.)*, 2012, **48**, 10334-10336.
80. T. J. J. Whitehorne and F. Schaper, *Inorg. Chem.*, 2013, **52**, 13612-13622.
81. T. J. J. Whitehorne and F. Schaper, *Can. J. Chem.*, 2014, **92**, 206-214.
82. K. S. Kwon, J. Cho, S. Nayab and J. H. Jeong, *Inorg. Chem. Commun.*, 2015, **55**, 36-38.
83. J. Cho, S. Nayab and J. H. Jeong, *Polyhedron*, 2016, **113**, 81-87.
84. S. H. Ahn, M. K. Chun, E. Kim, J. H. Jeong, S. Nayab and H. Lee, *Polyhedron*, 2017, **127**, 51-58.
85. K. S. Kwon, S. Nayab and J. H. Jeong, *Polyhedron*, 2017, **130**, 23-29.
86. M. K. Chun, J. Cho, S. Nayab and J. H. Jeong, *Bull. Korean Chem. Soc.*, 2017, **38**, 1527-1530.
87. S. Fortun, P. Daneshmand and F. Schaper, *Angew. Chem., Int. Ed.*, 2015, **54**, 13669-13672.
88. P. Daneshmand, A. van der Est and F. Schaper, *ACS Catal.*, 2017, **7**, 6289-6301.
89. P. Daneshmand, S. Fortun and F. Schaper, *Organometallics*, 2017, **36**, 3860–3877.
90. A. W. Addison, T. N. Rao, J. Reedijk, J. van Rijn and G. C. Verschoor, *J. Chem. Soc., Dalton Trans.*, 1984, DOI: 10.1039/DT9840001349, 1349-1356.
91. J. M. Fernández-G, J. Xochitiotzi-Flores, S. Hernández-Ortega, V. Gómez-Vidales and M. Del Rocío Patiño-Maya, *J. Coord. Chem.*, 2010, **63**, 2132-2145.
92. G. C. Percy and D. A. Thornton, *J. Inorg. Nucl. Chem.*, 1972, **34**, 3369-3376.
93. C. R. Groom, I. J. Bruno, M. P. Lightfoot and S. C. Ward, *Acta Crystallogr., Sect. B: Struct. Sci.*, 2016, **72**, 171-179.
94. J. U. Ahmad, M. T. Räisänen, M. Nieger, M. R. Sundberg, P. J. Figiel, M. Leskelä and T. Repo, *Polyhedron*, 2012, **38**, 205-212.
95. A. Mrutu, A. C. Lane, J. M. Drewett, S. D. Yourstone, C. L. Barnes, C. M. Halsey, J. W. Cooley and J. R. Walensky, *Polyhedron*, 2013, **54**, 300-308.
96. V. T. Kasumov, F. Köksal and Y. Zeren, *Spectrochimica Acta Part A: Molecular and Biomolecular Spectroscopy*, 2006, **63**, 330-336.
97. J. V. Singh, B. P. Baranwal and R. C. Mehrotra, *Z. Anorg. Allg. Chem.*, 1981, **477**, 235-240.
98. S. Mondal, S. M. Mandal, T. K. Mondal and C. Sinha, *Spectrochimica Acta Part A: Molecular and Biomolecular Spectroscopy*, 2015, **150**, 268-279.
99. G. N. Ledesma and S. R. Signorella, *Tetrahedron Lett.*, 2012, **53**, 5699-5702.
100. R. V. Stevens and G. S. Bisacchi, *J. Org. Chem.*, 1982, **47**, 2393-2396.
101. J. Uddin Ahmad, M. Nieger, M. R. Sundberg, M. Leskelä and T. Repo, *Journal of Molecular Structure*, 2011, **995**, 9-19.
102. X. Wang, K. Q. Zhao, Y. Al-Khafaji, S. Mo, T. J. Prior, M. R. J. Elsegood and C. Redshaw, *Eur. J. Inorg. Chem.*, 2017, **2017**, 1951-1965.
103. G. Alesso, M. Sanz, M. E. G. Mosquera and T. Cuenca, *Eur. J. Inorg. Chem.*, 2008, **2008**, 4638-4649.
104. M. Save, M. Schappacher and A. Soum, *Macromol. Chem. Phys.*, 2002, **203**, 889-899.
105. S. Yamada, H. Nishikawa and E. Yoshida, Vienna, 1964.
106. T. Hatsue, O. Kazuhide, T. Akira and Y. Shoichiro, *Bull. Chem. Soc. Jpn.*, 1979, **52**, 3522-3527.
107. K. Yamanouchi and S. Yamada, *Bull. Chem. Soc. Jpn.*, 1976, **49**, 163-168.
108. J. M. Fernández-G, O. L. Ruíz-Ramírez, R. A. Toscano, N. Macías-Ruvalcaba and M. Aguilar-Martínez, *Transition Metal Chemistry*, 2000, **25**, 511-517.
109. L. G. Cronenberger, Mrs. T.; Pacheco, H.; Pillon, D. , *Chimica Therapeutica*, 1968, **3**, 87-99.

View Article Online
DOI: 10.1039/C8DT02140F

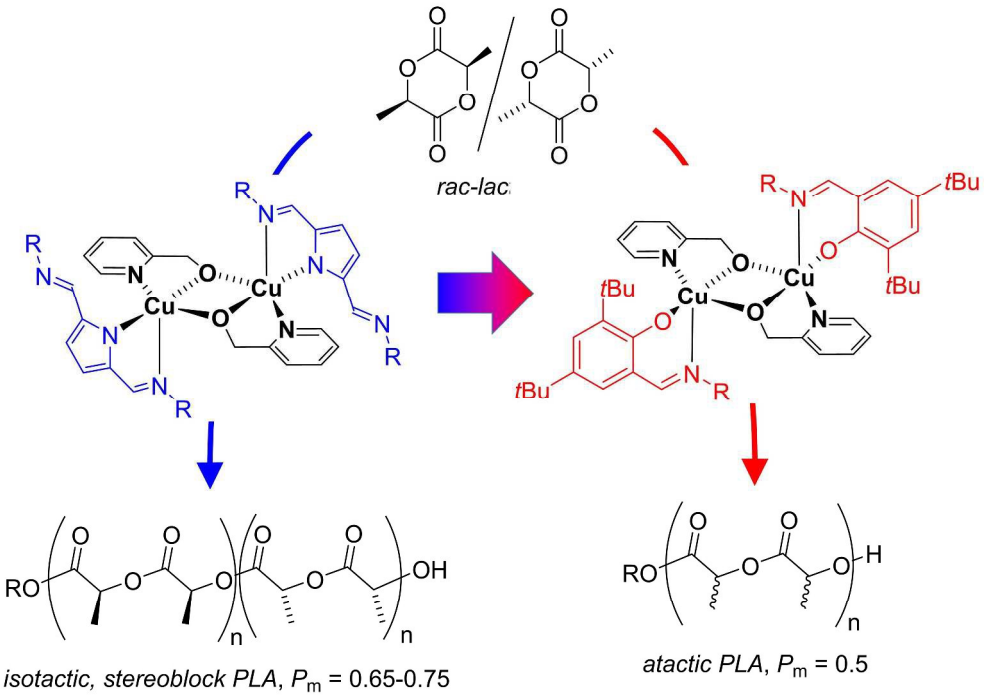

329x233mm (300 x 300 DPI)